ACS APPLIED MATERIALS & INTERFACES

LETTER

www.acsami.org

TiO_2 Fibers Enhance Film Integrity and Photovoltaic Performance for Electrophoretically Deposited Dye Solar Cell Photoanodes

Leyla Shooshtari,[†] Masoud Rahman,[*,‡] Fariba Tajabadi,[†] and Nima Taghavinia[*,†,‡]

[†]Physics Department, Sharif University of Technology, Tehran 14588, Iran.

[‡]Institute for Nanoscience and Nanotechnology, Sharif University of Technology, Tehran 14588, Iran.

Supporting Information

ABSTRACT: Nanoparticulated TiO_2 fibers as one-dimensional long structures were introduced into TiO_2 P25 nanoparticle films using coelectrophoretic deposition. This prevented the usual crack formation occurring in wet coatings, and resulted in less porosity and higher roughness factor of the films that provided more favorable conditions for electron transport. The films used as the photoanode of a dye solar cell (DSC) produced 65% higher photovoltaic efficiency. TiO_2 fibers can be excellent binders in single-step, organic-free electrophoretic deposition of TiO_2 for DSC photoanode.

KEYWORDS: electrophoretic deposition, TiO_2 fibers, dye solar cells, crack, porosity

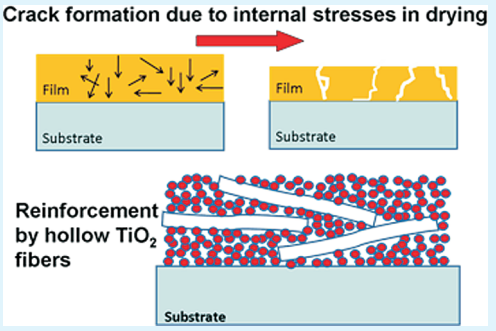

1. INTRODUCTION

The photoanode of a conventional dye sensitized solar cell (DSC) is a mesoporous TiO_2 film deposited from a viscous paste using doctor blade or screen printing. The TiO_2 paste contains organic additives which control the viscosity and prevent the crack formation. In order to decompose these organic additives, high temperature treatment (~450 °C) is required.[1] This high-temperature requirement restricts the application of these methods for flexible plastic substrates, which demand low temperature processes. Electrophoretic deposition (EPD) has been proposed as an alternative approach.[2−5] EPD can easily deposit nanoparticulated films with controllable film-thickness in one-step, with no need for organic binders. It also offers advantages such as multicomponent deposition,[6] site selective deposition, and no limitation on the shape of the substrate. This has initiated the use of EPD in fabrication of plastic-based DSCs.[4,7]

Nevertheless; a major challenge for EPD of thick films is the formation of cracks, mainly appearing during the evaporation of residual solvent inside the film which causes film shrinkage.[8−11] The disintegrated film demonstrates inferior electron transport properties. In addition, EPD normally creates films with too much porosity due to electrical repulsion of the particles. High porosity results in too many dead ends in the microstructure, which is detrimental to electron transport.[12]

Mechanical compression is one of the approaches to decreases the porosity and cracks in EPD films.[13,14] It also enhances the interparticle connections, resulting in better electron diffusion.[15,16] Multistep EPD with intermediate thermal cycle has also been employed to decrease the shrinkage stresses.[8] Inclusion of binders and geometrically long reinforcing structures has also proved useful in crack reduction. Binders are mainly polymers which in some cases are dispersants too. The presence of binders results in the enhancement of adherence and strength of films.[17] Jarernboon et al.[18] reported that addition of small quantity of multiwall carbon nanotubes (MWCNT) in the TiO_2 suspension significantly reduced the film cracks. However, the chemical bonding between MWCNT and TiO_2 nanoparticles is essential and requires surface modification of MWCNT.

Although the above-mentioned approaches have proved efficient toward crack reduction, their application is limited. The binders still have to be removed by high-temperature treatment and the MWCNTs may decrease the transparency of the photoanode or interfere in the recombination rate and conduction band energy level of photoanode in DSCs. The application of Mechanical pressing is also limited due to the uniformity of distribution of pressure inside the film as well as technical challenges for application on large modules.

Here, we have introduced nanoparticulated hollow TiO_2 fibers as reinforcing structures, into a TiO_2 nanoparticle film using coelectrophoretic deposition. We showed that TiO_2 fibers enhance the integrity of the film, as well as improve the photovoltaic performance of the cells. The reinforcing action of these fibers due to their long geometry can resist the shrinkage stresses of drying process. The fibers being composed of TiO_2 nanostructures make no adverse electronic or optical effect as other reinforcing binders. The influence of fibers on film morphology and their effect on the final DSC performance were investigated in this paper.

Received: November 30, 2010
Accepted: February 15, 2011
Published: February 22, 2011

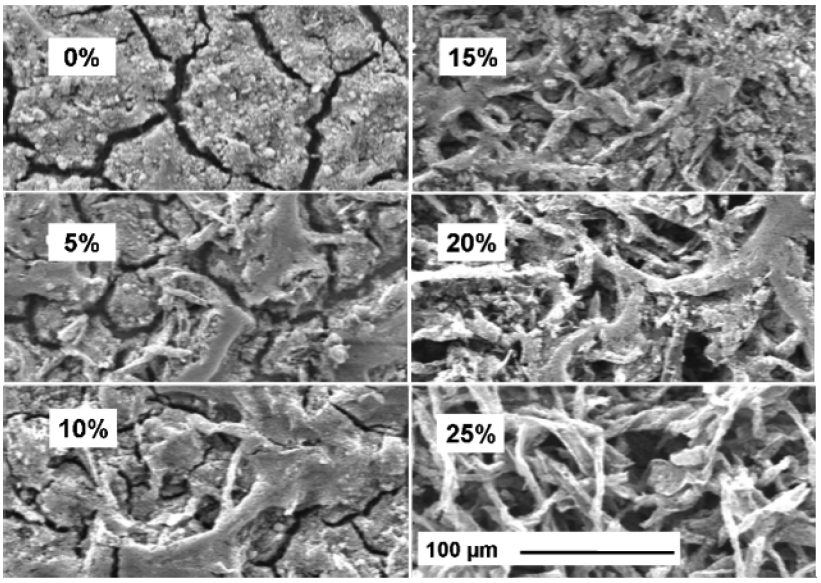

Figure 1. SEM images of the films prepared from the EPD sols of 0− 25% fiber contents.

2. EXPERIMENTAL METHOD

Nanoparticulated TiO_2 fibers were synthesized using layer-by-layer (LbL) self-assembly of TiO_2 nanoparticles on cellulose fibers as template, followed by thermal removal of the template at 500 °C for 4 h. LbL process consisted of 5 cycles of sequential deposition of TiO_2 nanoparticles (1 wt % sol, size =30 nm, ζ= −50 mV, pH 7),[19,20] and polydiallyldimethyl ammonium chloride (PDDA, MW: 100 K-200 K, Sigma-Aldirch, 0.02 M aqueous, pH 8) on cellulose fibers.

The ethanolic electrophoresis suspension was prepared according to the previous report by Zaban group.[2] It employed iodine, acetone and water as charging agents and Degussa P25 TiO_2 nanoparticles. Six solutions with the fiber-to-total-TiO_2 weight percentages of 0, 5, 10, 15, 20, and 25% were prepared.

EPD of TiO_2 fiber−nanoparticle films was performed at 10 V for 90 s, at 1 cm spacing between two electrodes. FTO glasses (15 Ω/□, Dyesol) as the substrate were coated first by a TiO_2 blocking layer (40 mM $TiCl_4$ solution, 70 °C, 30 min) prior to EPD. The samples were finally sintered at 500 °C for 1 h. The prepared composite films on FTO/glass were employed to fabricate solar cells by loading dye (N719, Dyesol) and using high performance electrolyte (EL-HPE, Dyesol) and 30 μm Surlyn spacer. The counter electrode was prepared on a perforated FTO-glass according to previously reported methods.[21]

The films were characterized using Brunauer−Emmet−Teller method (BET, Belsorp mini II), scanning electron microscopy (SEM, Philips-XL30) and X-ray diffraction (XRD, Philips PW1800). The active surface area of films was determined by dye-loading in 3 mL of NaOH (0.1 M in DI water) and estimating the concentration of dye using absorption measurements (PerkinElmer, Lambda 25). The DSC performance was evaluated in AM1.5 simulated light ((Luzchem-Solar) using a potentiostat/galvanostat (IVIUM, Compactstat).

3. RESULTS AND DISCUSSION

The EPD films of nanoparticles (without fibers) are cracked after preparation. The sizes of cracks are scaled with the thickness of the film (see the Supporting Information, Figure S1), as was already observed.[22] Introducing fibers in the film apparently enhances the integrity of films and reduces cracks, as shown in Figure 1. Undamaged fibers, almost parallel to the surface, with length of more than 100 μm and diameter of about 3−5 μm are observed together with the continuous deposit of nanoparticles. It seems that the nanoparticles have high tendency to adhere to the fibers (see the Supporting Information, Figure S2). This may lead to strong attachment of fibers to the film from multiple points and make the fibers as reinforcing components, resisting against the shrinkage forces and cracking during drying.

It is qualitatively evident from the SEM images that the quantity of fibers in the films is more than their nominal ratio in the EPD sol. This is quantitatively shown in Figure 2a, where it is demonstrated that the fiber content in the film is almost twice that in the EPD sol. The fiber content in the films was estimated by measuring the anatase content of films using XRD peak intensities (see the Supporting Information, Figure S3). Pure P25 films contain 81% anatase phase and 19% rutile phase, while addition of pure anatase fibers increases the total anatase content of the film in a linear way. The higher rate of deposition of fibers could be related to their lower detachment from the film which is caused by multiple-point bonding of fiber to the film compared with nanoparticles with lower bonding sites with the film. and/or geometrical factors affecting the electrophoretic mobility. Besides, fibers show larger ion adsorption, which could increase their deposition rate, as demonstrated by sol conductivity measurements (see the Supporting Information, Figure S4). This higher ion adsorption of fibers is due to their larger surface area, which is confirmed by BET measurements. According to BET measurements the surface area of fibers and P25 nanoparticles are 62.4 and 50 m^2/g, respectively.

In identical EPD conditions, up to 20% more TiO_2 is deposited on the substrate when fibers are present in the EPD sol, as demonstrated in Figure 2b. This is partly due to higher deposition rate of fibers. Nevertheless, we observed that the film thickness is almost identical for films with and without fibers. This implies that fibers cause denser films with lower porosity. The films porosity, obtained by comparing SEM thickness with mass thickness, is shown in Figure 2c. There is an evident decrease in the porosity which is favored in terms of electron transport in DSCs. This porosity reduction can be related to the crack reduction as well as flexibility of the fibers which helps them accommodate in the film densely. In the mean time, the

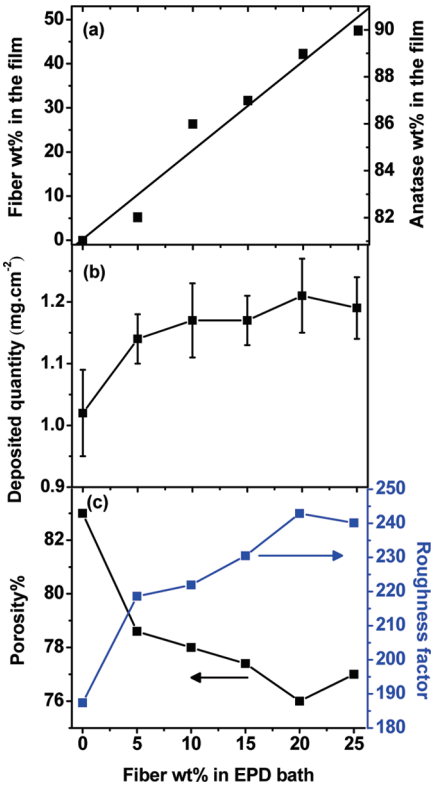

Figure 2. Morphological aspects of the films. (a) The fiber content in the film versus the fiber content in the EPD sol. The values are estimated from the anatase content of films measured using ratio of XRD peak intensities, shown as the right axis. (b) The deposited quantity of TiO_2 in terms of fiber content in the EPD sol. (c) Porosity and roughness factor of the films.

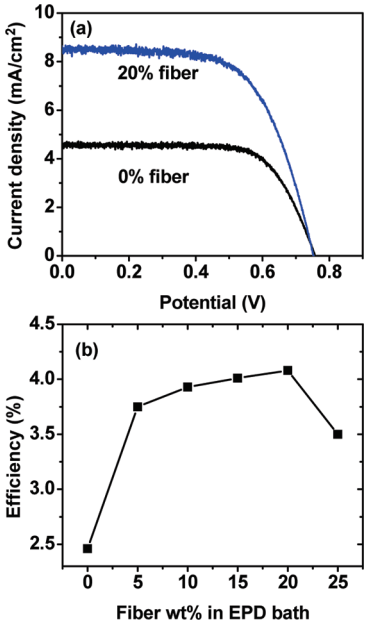

Figure 3. Photovoltaic performance of the cells employing the films containing fibers. (a) The J-V curves for films with 0% and 20% fiber content, and (b) The variation of cell efficiency versus fiber content.

roughness factor (ratio of active surface area to geometrical surface area) is increased for up to 30%. Apart from the larger amount of TiO_2 deposited in the presence of fibers, the higher BET surface area of fibers compared to nanoparticles leads to larger roughness factors.

Figure 3 shows the photovoltaic performance of the DSCs. The addition of fibers has a major improvement in the current density of cells, whereas V_{oc} is not highly affected. The comparison between samples with 0 and 20% fiber shows that the efficiency is enhanced up to 65%. This is partly due to about 30% increase in the dye loading. However, the effect of dye loading on efficiency is nonlinear and should be much less than 30%. The rest can be attributed to the light scattering by fibers, which produces better light harvesting, and/or improved electron transport properties due to the presence of fibers. More study on this issue is in progress.

4. CONCLUSION

TiO_2 fibers that were introduced into the nanoparticle films by coelectrophoretic deposition enhanced the film integrity by reducing the cracks and producing denser films. This is a more ideal condition as a DSC photoanode. TiO_2 fibers proved excellent as binders in the EPD of TiO_2 nanoparticles, which may facilitate single step, organic free deposition of DSC photoanodes.

■ ASSOCIATED CONTENT

Supporting Information. The role of electrophoresis time and voltage on the crack formation and film detachment (Figure S1); strong attachment of nanoparticles to the fibers (Figure S2); the XRD spectra of films with varying fiber content (Figure S3); and the higher ion adsorption of fibers duet to their higher surface area (Figure S4) (PDF). This material is available free of charge via the Internet at the http://pubs.acs.org.

■ AUTHOR INFORMATION

Corresponding Author

*rahman@ncl.sharif.edu (M.R.); taghavinia@sharif.edu (N.T.).

■ REFERENCES

(1) Ito, S.; Murakami, T. N.; Comte, P.; Liska, P.; Grätzel, C.; Nazeeruddin, M. K.; Grätzel, M. *Thin Solid Films* **2008**, *516*, 4613–4619.
(2) Grinis, L.; Dor, S.; Ofir, A.; Zaban, A. *J. Photochem. Photobiol., A* **2008**, *198*, 52–59.
(3) Zhao, L.; Yu, J.; Fan, J.; Zhai, P.; Wang, S. *Electrochem. Commun.* **2009**, *11*, 2052–2055.
(4) Yum, J.; Kim, S.; Kim, D.; Sung, Y. *J. Photochem. Photobiol., A* **2005**, *173*, 1–6.
(5) Tan, W.; Yin, X.; Zhou, X.; Zhang, J.; Xiao, X.; Lin, Y. *Electrochim. Acta* **2009**, *54*, 4467–4472.
(6) Cho, J.; Schaab, S.; Roether, J. A.; Boccaccini, A. R. *J. Nanopart. Res.* **2008**, *10*, 99–105.
(7) Miyasaka, T.; Kijitori, Y. *J. Electrochem. Soc.* **2004**, *151*, A1767–A1773.
(8) Chang, H.; Chen, T. L.; Huang, K. D.; Chien, S. H.; Hung, K. C. *J. Alloys Compd.* **2010**, *504*, S435–S438.
(9) Scherer, G. W. *J. Am. Ceram. Soc.* **1990**, *73*, 3–14.
(10) Chiu, R. C.; Garino, T. J.; Cima, M. J. *J. Am. Ceram. Soc.* **1993**, *76*, 2257–2264.
(11) Chiu, R. C.; Cima, M. J. *J. Am. Ceram. Soc.* **1993**, *76*, 2769–2777.
(12) Benkstein, K. D.; Kopidakis, N.; Lagemaat, J. van de; Frank, a J. *J. Phys. Chem. B* **2003**, *107*, 7759–7767.
(13) Dittrich, T.; Ofir, A.; Tirosh, S.; Grinis, L.; Zaban, A. *Appl. Phys. Lett.* **2006**, *88*, 182110.
(14) Chen, H.-W.; Hsu, C.-Y.; Chen, J.-G.; Lee, K.-M.; Wang, C.-C.; Huang, K.-C.; Ho, K.-C. *J. Power Sources* **2010**, *195*, 6225–6231.

(15) Ofir, A.; Dittrich, T.; Tirosh, S.; Grinis, L.; Zaban, A. *J. Appl. Phys.* **2006**, *100*, 074317.
(16) Dor, S.; Rühle, S.; Ofir, A.; Adler, M.; Grinis, L.; Zaban, A. *Colloids Surf., A* **2009**, *342*, 70–75.
(17) Zhitomirsky, I. *Adv. Colloid Interface Sci.* **2002**, *97*, 279–317.
(18) Jarernboon, W.; Pimanpang, S.; Maensiri, S.; Swatsitang, E.; Amornkitbamrung, V. *J. Alloys Compd.* **2009**, *476*, 840–846.
(19) Hosseini, Z.; Taghavinia, N.; Sharifi, N.; Chavoshi, M.; Rahman, M. *J. Phys. Chem. C* **2008**, *112*, 18686–18689.
(20) Rahman, M.; Taghavinia, N. *Eur. Phys. J. Appl. Phys.* **2009**, *48*, 10602.
(21) Ito, S.; Chen, P.; Comte, P.; Nazeeruddin, M. K.; Liska, P.; Péchy, P.; Grätzel, M. *Prog. Photovolt: Res. Appl.* **2007**, *15*, 603–612.
(22) Jarernboon, W.; Pimanpang, S.; Maensiri, S.; Swatsitang, E.; Amornkitbamrung, V. *Thin Solid Films* **2009**, *517*, 4663–4667.